2023 IEEE International Conference on Robotics and Automation (ICRA 2023)
May 29 - June 2, 2023. London, UK

A hydraulic soft robotic detrusor based on an origami design

Simone Onorati[#], Federica Semproni[#], Linda Paternò[#], *Member, IEEE*, Giada Casagrande, Veronica Iacovacci*, *Member, IEEE*, and Arianna Menciassi, *Senior Member, IEEE*

***Abstract* — As a permanent solution for patients who cannot contract their urinary bladder, an artificial detrusor muscle appears a higher outcome approach compared to current sacral neurostimulators featured by severe long-term side effects.**

In this paper, a novel soft robotic detrusor is presented to overcome the limitations of the state-of-the-art solutions. It is based on two identical origami-based hydraulic actuators, which completely surround the bladder and contract upon water aspiration. Design, manufacturing, and experimental characterization both in terms of contraction capabilities and voiding efficiency on ex vivo swine bladders are reported for two different origami geometries, as well as a proof-of-concept implementation of an autonomous driving circuit as control unit.

Results from assisted urination tests outlined very good performances proving an active voiding efficiency of the hydraulic soft robotic detrusor equal to 84.8% ± 7.4% in simulated environment.

I. Introduction

Worldwide, millions of people suffer from neurological and non-neurological disorders that can impair controlled bladder emptying capabilities (e.g., spinal injuries and detrusor aging) [1]. Neurostimulators have been proposed to reactivate the associated neural pathways, but they feature severe long-term side effects [2].

Continence maintenance appears crucial when restoring or supporting urinary system functions. Active artificial bladders should allow for both collecting urinary fluids and controlled voiding when needed. In the past years, artificial urinary sphincters have been proposed with few designs reaching the market, whereas very few fully artificial bladders endowed with active voiding are present in the state-of-the-art [3]–[5]. Recently, the authors exploited soft hydraulic actuators to develop a novel concept of active artificial bladder [6] that aims at overcoming the encumbrance and low compliance of previous mechatronic designs for patients in which the native bladder was removed [7].

In patients preserving the native bladder but not able to control it, artificial detrusor systems might act as an alternative solution, although sparsely approached by researchers. Thermoresponsive hydrogels [8] and shape memory alloys (SMA) [9] have been proposed to mimic the natural detrusor muscle and enable native bladder contraction. However, these systems are devised for small animals bladders (volume in the range of 0.2–50 mL). In addition, the heating-related side effects associated with SMA and the slow dynamics of thermoresponsive hydrogels make it necessary to look for new approaches to cope with native bladder voiding through artificial detrusors. In this direction, using a robotic approach to develop implantable devices able to support or restore lost organ functionalities opens up new venues towards efficient solutions [10], [11]. Recently, a soft robotic magnetic detrusor has been proposed and successfully tested on pigs [12], thus representing an important step forward in the field of implantable biorobotic organs and detrusor mimicking. Nevertheless, the proposed design exerts a compressive action still far from mimicking the isotropic contraction of the natural detrusor and calls for an external control source (e.g., a magnet) for on-demand activation. Therefore, the quest for a fully implantable artificial detrusor mimicking the natural counterpart while guaranteeing safe and efficient implantation, still persists.

Pneumatic [13], electroactive polymer [14], and hydraulic actuators [5] have been successfully proposed in the literature to reproduce muscle functions in impaired organs. In light of their muscle-like operation, fluidic actuators appear particularly intriguing for a novel robotic detrusor. In the family of fluidic actuators, hydraulic solutions look promising compared with pneumatic ones. In fact, by using biocompatible liquids, a higher safety can be targeted in the implantable systems while also reducing the risk of bursts [15]. Furthermore, liquids feature lower compressibility and a higher force-to-volume ratio [16].

In this paper, a novel hydraulic soft robotic detrusor is proposed for controlled bladder voiding. It is composed of two identical semi-ellipsoidal fluidic actuators embracing the natural bladder. Inspired by vacuum-driven designs featured by high contraction performances, each actuator consists of a water-filled chamber made of a soft silicone skin and enclosing a flexible acetate origami skeleton with a waterbomb pattern. The origami guides the change from a curved to a flat configuration when depressurization is applied, thus compressing the natural bladder and allowing for voiding. This origami pattern has already been exploited in shape-morphing structures [17], soft grippers [18], and self-expanding stents [19], demonstrating a volume contraction capability up to 90% [17]. However, the concept was never used for medical applications or implantable robotic organs.

Two origami sizes were devised and tested as core structure of the fluidic actuators both in terms of contraction ratio and produced bladder voiding efficiency. The design, fabrication procedure, and setup used for the characterization of the fluidic soft robotic detrusor – both as a single actuator and when installed on a natural bladder – are described in Section II. Here a first implementation of a miniaturized driving circuit for the future implant of the device is also presented. Section III reports the results of the geometrical characterization of the actuators, as well as their performance as detrusor during ex vivo tests. Last, in Section IV we recapitulate the added value of this work in the field of implantable urinary prostheses.

# These authors contributed equally to the work.

This work was supported by INAIL, the Italian National Institute for Insurance against Work-related Injuries (non-commercial entity), within the PR19-CR-P2 BioSUP (BIOnic Solutions for Urinary impaired People) project framework.

All authors are with The BioRobotics Institute, Scuola Superiore Sant'Anna, Pontedera (Pisa), Italy.

V. Iacovacci is also with the Department of Mechanical and Automation Engineering, The Chinese University of Hong Kong, Hong Kong, China.

* Corresponding author: veronica.iacovacci@santannapisa.it

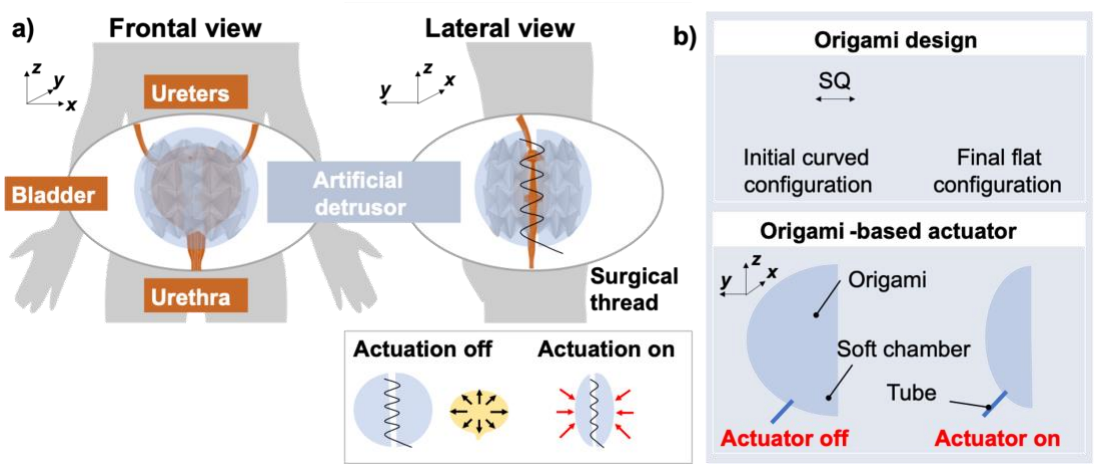

Figure 1. (a) Design of the fluidic soft robotic detrusor and illustration of its operating principle to void the human bladder. (b) Design of a single fluidic actuator included in the soft robotic detrusor. The actuator is constituted by an origami with a waterbomb pattern, enclosed in a semi-ellipsoidal fluid-filled chamber made of a soft but inextensible silicone skin. The actuation principle is based on the depressurization of the chamber which produces the origami contraction, thus changing the actuator configuration from an initial curved shape to a final flat one. SQ represents the side of waterbomb pattern cell square in the origami design.

II. Materials and Methods

A. Working principle and design overview

The proposed soft robotic detrusor is composed of two identical fluid-driven actuators, bound together to embrace the bladder and the ureters/urethra (Figure 1a). This design was chosen to allow for straightforward surgical implantation of the prosthesis around the bladder, without the need for temporary resection of the three urinary ducts. The two actuators can be sewn together by a biostable surgical thread once positioned in the patient's body. Each actuator consists of: *(i)* a waterbomb-pattern origami as core structure, obtained by folding a grid of cell squares with SQ side; *(ii)* a semi-ellipsoidal chamber – made of a soft material yet with low stretchability – filled with water and enclosing the origami; *(iii)* a fluidic tube, which connects the soft chamber to a miniaturized fluidic circuit (Figure 1b and Supplementary Video). The actuation principle relies on the capability of the waterbomb origami to switch from an initial curved to a final flat configuration through the contraction of its crests. This switch is activated by depressurizing and drawing water out from the soft actuators. The origami shape switch produces a uniform and distributed contraction force over the embraced native bladder.

The use of low-stretchability materials for both the skin and the origami is required for a proper actuator contraction. In fact, since the skins cannot fully stretch, the soft chamber pulls the adjacent crests of the origami one towards the other during depressurization. Conversely, a highly stretchable material would extend in the free space among the crests of the origami, thus hindering the contraction movement.

In order to identify the best actuator design in terms of contraction and bladder voiding efficiency, two different origami unit sizes (the side of the cell square, SQ in Figure 1b) were investigated. In particular, two detrusor types were developed: the SQ3 type (origami skeleton of 6 x 4 square cells with a side of 3 cm) and the SQ2 type (skeleton of 8 x 6½ squares with a side of 2 cm) (Figure 2).

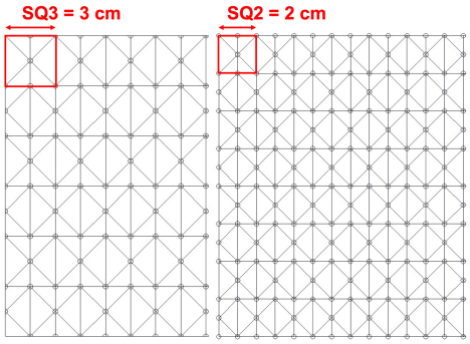

Figure 2. Design of the waterbomb pattern of the origami before folding: SQ3 (left) and SQ2 (right) type. Small circular areas around each vertex were cut to prevent soft chamber punching in the actuator.

Table 1 reports the geometrical features, weight, and inner water volume at the initial rest state (actuators off) of the two detrusor types (each constituted by two fluidic actuators). The geometrical dimensions are shown in Figure 3.

Table 1. Parameters of the two detrusor types (each constituted by two actuators) in their initial rest state (actuators off).

Parameter	SQ3 model	SQ2 model
Silicone skin thickness	1 mm	0.5 mm
Single actuator length (l_{1i} in Fig. 3)	~ 120 mm	~ 110 mm
Single actuator height (l_{2i} in Fig. 3)	~ 40 mm	~ 35 mm
Single actuator width (l_{3i} in Fig. 3)	~ 75 mm	~ 65 mm
Weight of full detrusor (two actuators)	~ 110 g	~ 80 g
H_2O operative volume of each actuator	~ 70 mL	~ 60 mL

B. Detrusor fabrication

The fabrication of the fluidic soft robotic detrusor comprised four different steps (Figure 4): (*i*) manufacturing of the origami with waterbomb pattern; (*ii*) manufacturing of the semi-ellipsoidal soft skins of the chamber; (*iii*) assembly of a single actuator; (*iv*) assembly of two actuators to complete the soft robotic detrusor.

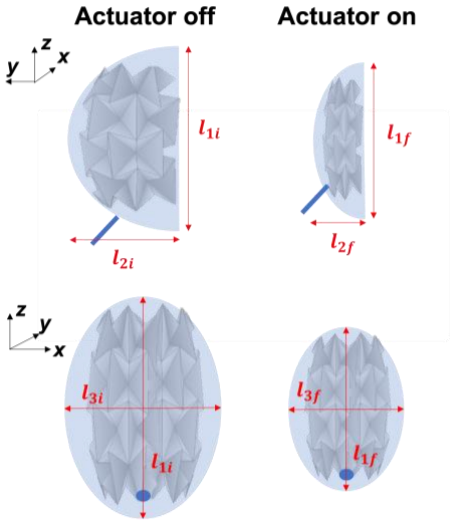

Figure 3. Main dimensions of the actuator in the rest state (actuator off) and when actuated (actuator on).

The origami was realized by laser cutting the waterbomb pattern on a semirigid sheet of 0.16 mm thick acetate (EVA), stacked with a soft sheet of 0.07 mm thick polyethylene (LDPE) by a layer of double-sided tape (Figure 4a). LDPE and tape were used to allow for an improvement of the origami durability, since they guarantee the structure integrity also in case of EVA sheet damages. Different laser powers were exploited to cut the origami contour and to slightly engrave the folding lines without affecting the integrity of the sheets.

Each soft chamber was made by gluing two semi-ellipsoidal skins, made of soft but low-stretchability material. In particular, the skins were obtained by embedding a medical gauze in silicone rubber (Ecoflex™ 00-30, Smooth-On, Inc., USA) using a 3D-printed mold designed in SolidWorks (Figure 4b). For each skin, the gauze was fixed on the upper part of the mold and strewed completely with silicone. Then, silicone was put in the bottom part and the mold was closed. After silicone curing, the skin was extracted.

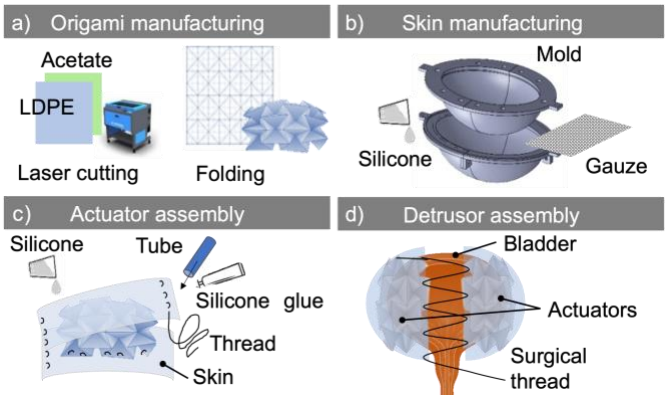

Figure 4. Manufacturing of origami and skins, assembly of a single actuator, and assembly of two actuators to obtain the soft robotic detrusor.

For the assembly of the actuator, the origami perimeter was sewed to the first skin which in turn was sewed to the second one (Figure 4c). Then, the actuator was sealed hermetically by pouring silicone all over the seams. A flexible tube was integrated with silicone glue (Sil-Poxy™, Smooth-On, Inc.).

Two actuators can be sewn tightly around the native bladder upon implantation to obtain the final fluidic soft robotic detrusor (Figure 4d).

C. Experimental characterization

Actuators contraction performance. The semi-ellipsoidal actuator was characterized in terms of contraction ratio along the x, y, and z axes (Figure 3) [20]:

$$\lambda_z = 1 - \frac{l_{1f} - l_{1i}}{l_{1i}} \quad (1)$$

$$\lambda_y = 1 - \frac{l_{2f} - l_{2i}}{l_{2i}} \quad (2)$$

$$\lambda_x = 1 - \frac{l_{3f} - l_{3i}}{l_{3i}} \quad (3)$$

In particular, the main dimensions and the inlet pressure of the actuator (P) were measured when drawing out the total water volume (i.e., 70 mL for SQ3 and 60 mL for SQ2, volumes were selected to enable proper filling of the chambers in the two designs) at steps of 10 mL. Water aspiration was provided by a motorized syringe pump (model NE-1010, New Era Pump Systems, Inc., USA) at flow rate of 50 mL/min. A differential pressure sensor (MPX5100DP, Freescale Semiconductor, Inc., USA), interfaced to an Arduino™ Mega 2560 connected to MATLAB™ R2021b, was used for recording pressure values, while the main dimensions of the actuators were measured with a caliper. For each detrusor type (SQ3 and SQ2), the characterization was repeated three times on each of the three different semi-ellipsoidal prototypes. The mean and standard deviation of the contraction ratios were computed.

Detrusor assistive voiding performances. The performances of the two fluidic soft robotic detrusors (SQ2 actuator composed of two SQ2 semi-ellipsoidal prototypes, and SQ3 actuator composed of two SQ3 semi-ellipsoidal prototypes) were tested ex vivo on three adult swine bladders, which show comparable sizes to the human bladder. The electro-hydraulic circuit used during these tests is depicted in Figure 5. It consists of two fluidic lines. *Line 1* connects the syringe pump to the two detrusor actuators around the bladder and to a reservoir. An MPX5100DP differential pressure sensor was connected to the detrusor to monitor the inlet pressure of the actuators with respect to the environment. *Line 2* connects the natural bladder to a collection pool via a second MPX5100DP sensor used to monitor the intravesical pressure, and a two-way valve surrogating the urinary sphincter. The pool is placed on an electronic scale (WLC 2/A2, Radwag, Poland), which can record the ejected urine weight for deriving the ejected volume over time $V(t)$.

After the detrusor actuators were filled by the syringe, the ex vivo bladder was filled with water from the urethra by means of a manual syringe. The bladder filling was stopped at a volume (V_u) corresponding to an intravesical pressure of 3.0 kPa. This guarantees not overcoming the threshold of 4.3 kPa, which represents the natural trigger for the self-urination reflex in healthy humans [21].

The bladder was tested in the horizontal configuration, which represents the most unfavorable scenario when micturition is not assisted by gravity, as in bed-ridden patients. The artificial sphincter was opened as soon as the aspiration command was sent to the syringe connected to the two actuators, and the recording started. The recording was

ended once the weight increment in the last 50 samples (corresponding to ~ 8 s on the used laptop) was lower than 0.03 g.

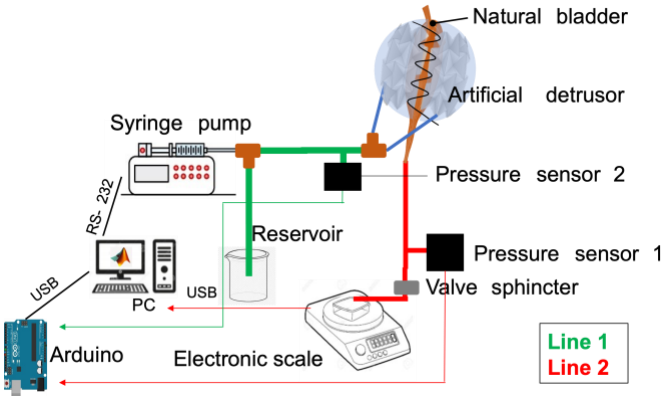

Figure 5. Experimental setup for the ex vivo characterization of the soft robotic detrusors. *Line 1* connects the syringe pump to the detrusor, *Line 2* connects the natural bladder to a collection pool on the electronic scale.

The performance of the SQ2 and SQ3 actuators were compared in terms of bladder voiding efficiency. In order to assess the advantages produced by an active fluidic soft robotic detrusor, the voiding efficiency was estimated repeating the tests also for bladders surrounded by non-active detrusors (i.e., assessing the contribution of the detrusor weight in the micturition). To account for the organ biological variability, the tests were repeated on 3 different bladders and each configuration (i.e., passive and active) was tested 4 times. Micturition was evaluated in terms of: (*i*) Voiding Efficiency (VE [%]), i.e., the ratio of the ejected volume at the end of micturition and V_u; and (*ii*) Post-Voiding Residual volume (PVR [mL]), i.e., the urine volume in the bladder when the micturition was finished. A target VE for the active micturition process is 90%, while the PVR should stay below 50 mL [22].

D. Driving circuit design

A dedicated control unit was designed to drive the activation of the fluidic soft robotic detrusor (Figure 6).

Even if further miniaturization and more efficient power management will be needed in the future, this step paves the way to system implantation. The control unit is featured by two alternative hydraulic lines (i.e., yellow and blue in Figure 6), respectively to move water from the detrusor actuators to the reservoir (during the contraction phase, actuators on), and from the reservoir to the detrusor actuators (for restoring the initial rest state, actuators off). Each line comprises a micro-pump for liquids (SP 270 EC-L, Schwarzer Precision, Germany) and a miniaturized normally-closed electro-valve (Series 3, Parker Hannifin, USA). The output of an MPX5100DP differential pressure sensor is exploited to control the water flow. A powering circuit provides 5 V to the pumps and 12 V to the electro-valves and it is supplied with a battery of 7.4 V.

An Arduino™ Nano 3 microcontroller connected to MATLAB R2021b acts as a central control unit. Following a command from the PC, the aspiration line (yellow line in Figure 6) is activated, while the MPX5100DP pressure sensor monitors the depression in the actuators. When the set maximum vacuum pressure is read, the valve (yellow one in Figure 6) is shut and the pump stopped. A second command opens the second electro-valve and activates the corresponding micro-pump (blue line in Figure 6), which restores the waterbomb actuators to their initial rest state.

The control unit was exploited to depressurize a SQ3 detrusor prototype implanted around an ex vivo swine bladder in a human manikin. Voiding performances of the full system were measured also in presence of other ex vivo tissues simulating surrounding organs encumbrances. Both the test types, with and without other tissues, were repeated 3 times.

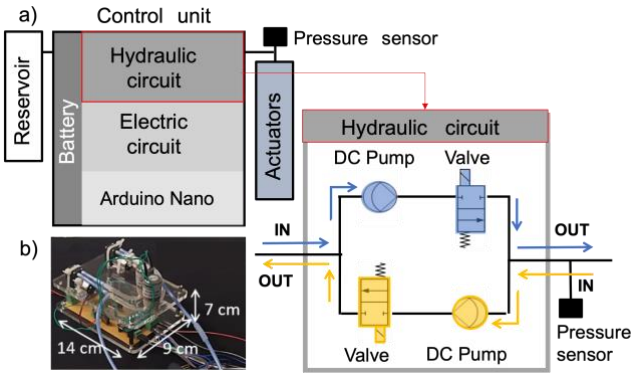

Figure 6. (a) Block diagram of the control unit of the fluidic soft robotic detrusor and scheme of its two hydraulic lines (blue: from the reservoir to the actuators; yellow: from the actuators to the reservoir). (b) Photo and size of the control unit.

III. Results

A. Actuator performance

Figure 7 show the contraction ratios along *x*, *y*, and *z* at different inlet absolute pressures of a single semi-ellipsoidal actuator with SQ3 (a) and SQ2 design (b), respectively. Given the different initial water volume of the two actuators at rest state (i.e., 70 mL for SQ3 and 60 mL for SQ2 design), seven pressure values were tested for SQ3 and six values for SQ2, each corresponding to a further water volume of 10 mL drawn out of the actuator.

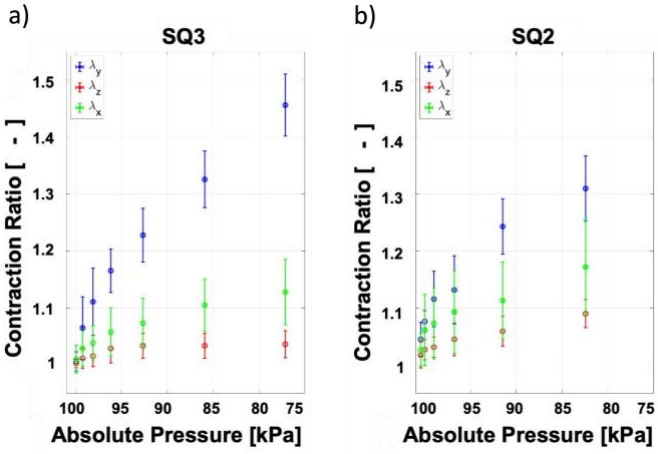

Figure 7. Experimental results of the contraction ratios along the *x*, *y*, and *z* axis of the actuator (λ_x, λ_y, λ_z) with respect to the inlet absolute pressure, for the SQ3 and SQ2 design, (a) and (b), respectively.

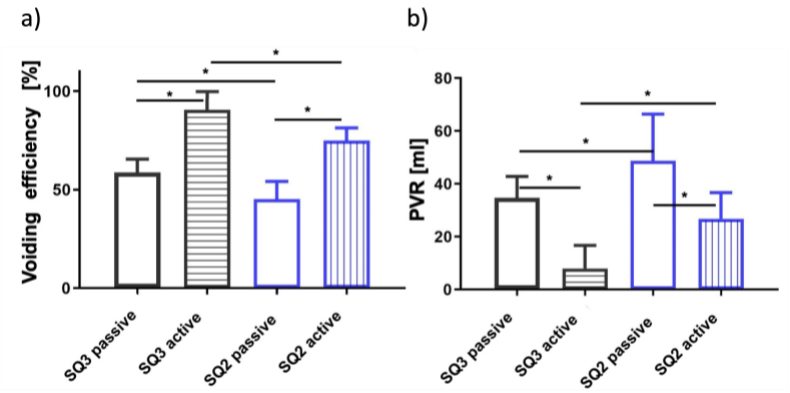

Figure 8. Experimental results of the micturition quality evaluated by: (a) Voiding Efficiency (VE), i.e., the ratio of the ejected volume at the end of urination and the bladder filling volume V_u; (b) Post-Voiding Residual volume (PVR), i.e., the urine volume in the bladder at the end of the micturition. Each parameter was tested on bladders surrounded by the fluidic soft robotic detrusor, placed horizontally, in the passive and active state, and for both SQ3 and SQ2 designs. Horizontal black bars with * indicate p-value < 0.05 between test pairs.

It can be noticed that for both actuator designs, the major contraction happens in the *y* direction, orthogonal to the base ellipse (Figure 3; max value: $\lambda_y = 1.46 \pm 0.06$ for SQ3 at $P = 77$ kPa and $\lambda_y = 1.31 \pm 0.06$ for SQ2 at $P = 82$ kPa); a significant compression happens also along the minor ellipse axis (max value: $\lambda_x = 1.13 \pm 0.06$ for SQ3 at $P = 77$ kPa and $\lambda_x = 1.17 \pm 0.08$ for SQ2 at $P = 82$ kPa); while only a slight contraction was observed along the major ellipse axis (max value: $\lambda_z = 1.04 \pm 0.02$ for SQ3 at $P = 77$ kPa and $\lambda_z = 1.09 \pm 0.02$ for SQ2 at $P = 82$ kPa). This difference in the three directions is related to the flattening property along *y* of the waterbomb pattern origami: it is featured by a tessellated convex shape that switches to a planar one when the actuator is activated. In addition, during actuation, the vertical crests of the tessellation get closer to each other in the *x* direction, thus causing a high value of λ_x.

When comparing SQ3 to SQ2 at the full volume aspiration (i.e., 0 mL inlet water, maximum depression), the former contracts slightly less along the lateral directions (*x, z*), but more along the *y* axis. This difference is thought to be due to the higher resistance to bending of the folds in the SQ2 origami design, which is composed of the same material thicknesses but has a higher density of folds.

B. Detrusor performance

Figure 8 presents the micturition quality parameters evaluated during the ex vivo tests. Experimental data showed promising results for both detrusor types, but particularly for SQ3 due to its higher contraction ratio (Figure 7). In this regard, with actuated detrusors, a VE equal to 91% and 75% was measured for SQ3 and SQ2, respectively. Furthermore, concerning PVR, a statistically significant difference between the two designs was found, with a mean value < 30 mL for SQ2 and even < 10 mL for SQ3.

Comparing the performances between the passive and active case of micturition, the VE and PVR are significantly better in the assisted urination both for SQ3 and SQ2 (*p*-value < 0.05): with the SQ3 model, VE increases by ~ 1.5 times and PVR decreases by ~ 4 times; with SQ2, VE increases by ~ 1.7 times and PVR decreases by ~ 1.8 times. Thus, we can confirm that adding actuation to the prosthetic detrusor, even if power-consuming, improves the micturition process and its controllability with respect to having only the weight of the half-detrusor (passive case) over the bladder easing the micturition.

C. Final system in simulated environment

The final prototype of the fluidic soft robotic detrusor, together with the miniaturized control unit, is shown in Figure 9. The SQ3 design, which featured higher efficiency on bench tests, was selected for more extensive investigations in a simulated environment and using the miniaturized electro-hydraulic circuit as control unit. The fluidic soft robotic detrusor was implanted around an ex vivo swine bladder and placed in a human manikin together with other ex vivo tissues simulating surrounding organs encumbrance (Supplementary Video).

Tests carried out in this simulated environment demonstrated an active ve equal to 84.8% ± 7.4%, quite comparable with one observed during bench tests.

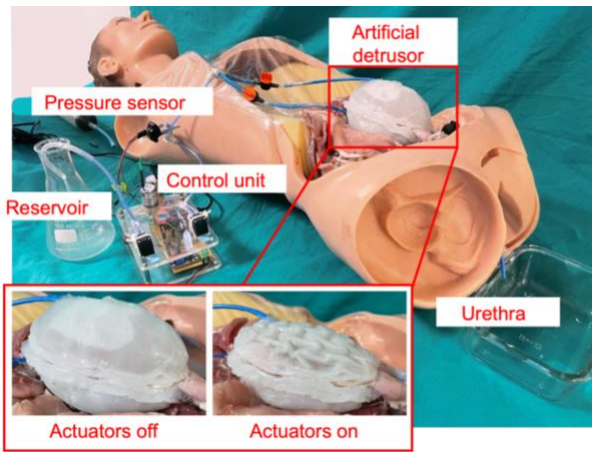

Figure 9. Final fluidic soft robotic detrusor with the miniaturized control unit. The prototype was mounted around an ex vivo swine bladder in a human manikin, with other ex vivo tissues around (some removed in this figure), to assess its voiding performances.

IV. Discussion and Conclusion

In the literature, using soft fluidic actuation for implantable prostheses is not a new concept (e.g., they are used in the cardiac field [23]). However, it was never explored for bladder voiding. In the present work, we proved the feasibility of using a hydraulic, origami-based soft actuator as

the building block for a robotic detrusor for controlled micturition. A large contraction stroke – required to produce an acceptable voiding efficiency of the bladder – was achieved by exploiting the waterbomb pattern origami: the maximum contraction ratios along the *y* direction of a single actuator are around 145% for the SQ3 origami and 130% for the SQ2, respectively. Such contraction ratios result comparable with the state-of-the-art solutions [17], [24], confirming the high strokes of the selected origami design.

Compared to the already proposed artificial detrusors, the fluidic approach proves attractive for its inherent safety: no abdominal tissues overheating as a side effect is present, and medium to low power consumption is needed. Thanks to the pushing force exerted on the bladder by the depressurization of the fluidic actuators, we could obtain both in ex vivo setup and in the simulated in vivo environment, VEs up to 90% (with SQ3 model) and PVRs below the clinical warning threshold of 50 mL. These results are notable compared to the other artificial detrusor solutions for natural bladder proposed in the literature. With the thermo-responsive hydrogel-based actuation [8], only modest urination was observed in vivo on rabbits (no VE and PVR are reported). In a recently developed SMA-based detrusor [25], a VE of 75% was achieved in vivo in mice. Additionally, the new soft robotic detrusor based on external magnetic coupling [12] showed a powerful actuation force throughout all the high shell contraction range, leading to VEs between 90% and 100%, and PVRs below 30 mL on in vivo porcine bladders. However, the activation of this system is not fully automated, and the shape of the active elements makes the compressive action not uniform on the bladder tissue.

Given the optimal performance of the proposed soft robotic detrusor design, future work will focus on a design optimization to furtherly enhance its performances and chronic implantability. In this sense, the design of the fluidic soft robotic detrusor made of two identical actuators can allow for minimally invasive implantation without the need for temporary resecting the ureters. However, to enable full implantability, the actuators operative fluid volume should be reduced, to allow for the housing of a service reservoir connected to the driving circuit [26]. In addition, we proposed and successfully tested a first version of an integrated electro-hydraulic driving circuit, that can allow for autonomous detrusor activation. However, further miniaturization and power consumption optimization have to be pursued in future works, toward a fully implantable compact solution. Although no ruptures of the soft chambers were observed during repeated tests on the same prototypes, long-term tests will be performed to assess the durability of the actuators.

Overall, the results reported in this paper represent a significant step forward in the field of implantable robots and pave the way to novel soft robotic systems for controlled bladder voiding.

REFERENCES

[1] Y. Kang *et al.*, 'Epidemiology of worldwide spinal cord injury: a literature review', *J. Neurorestoratology*, vol. 6, pp. 1–9, Dec. 2017, doi: 10.2147/JN.S143236.

[2] S. M. Yaiesh, A. Al-Terki, and T. F. Al-Shaiji, 'Neuromodulation in Urology: Current Trends and Future Applications', 2020. doi: 10.5772/intechopen.92287.

[3] T. Mazzocchi, L. Ricotti, N. Pinzi, and A. Menciassi, 'Magnetically Controlled Endourethral Artificial Urinary Sphincter', *Ann. Biomed. Eng.*, vol. 45, no. 5, pp. 1181–1193, May 2017, doi: 10.1007/s10439-016-1784-2.

[4] S. Hached, Z. Saadaoui, O. Loutochin, A. Garon, J. Corcos, and M. Sawan, 'Novel, Wirelessly Controlled, and Adaptive Artificial Urinary Sphincter', *IEEEASME Trans. Mechatron.*, vol. 20, no. 6, pp. 3040–3052, Dec. 2015, doi: 10.1109/TMECH.2015.2389254.

[5] 'AMS 800™ Artificial Urinary Sphincter', *www.bostonscientific.com*. https://www.bostonscientific.com/en-US/products/artificial-urinary-sphincter/ams-800-artificial-urinary-sphincter.html (accessed Sep. 08, 2022).

[6] G. Casagrande, M. Ibrahimi, F. Semproni, V. Iacovacci, and A. Menciassi, 'Hydraulic Detrusor for Artificial Bladder Active Voiding', *Soft Robot.*, p. soro.2021.0140, Jun. 2022, doi: 10.1089/soro.2021.0140.

[7] Z. Zhuo, H. Dan, L. Gensong, S. Ping, and P. Xining, 'Design of a Mechatronics Model of Urinary Bladder and Realization and Evaluation of Its Prototype', *Appl. Bionics Biomech.*, vol. 2019, pp. 1–9, Dec. 2019, doi: 10.1155/2019/9431781.

[8] X. Yang *et al.*, 'Soft Artificial Bladder Detrusor', *Adv. Healthc. Mater.*, vol. 7, no. 6, p. 1701014, 2018, doi: 10.1002/adhm.201701014.

[9] F. A. Hassani *et al.*, 'A 3D Printed Implantable Device for Voiding the Bladder Using Shape Memory Alloy (SMA) Actuators', *Adv. Sci.*, vol. 4, no. 11, p. 1700143, Nov. 2017, doi: 10.1002/advs.201700143.

[10] A. Menciassi and V. Iacovacci, 'Implantable biorobotic organs', *APL Bioeng.*, vol. 4, no. 4, p. 040402, Dec. 2020, doi: 10.1063/5.0032508.

[11] V. Iacovacci *et al.*, 'A fully implantable device for intraperitoneal drug delivery refilled by ingestible capsules', *Sci. Robot.*, vol. 6, no. 57, p. eabh3328, Aug. 2021, doi: 10.1126/scirobotics.abh3328.

[12] Y. Yang *et al.*, 'Magnetic soft robotic bladder for assisted urination', *Sci. Adv.*, vol. 8, no. 34, p. eabq1456, Aug. 2022, doi: 10.1126/sciadv.abq1456.

[13] E. T. Roche *et al.*, 'Soft robotic sleeve supports heart function', *Sci. Transl. Med.*, vol. 9, no. 373, p. eaaf3925, Jan. 2017, doi: 10.1126/scitranslmed.aaf3925.

[14] F. M. Weiss, H. Deyhle, G. Kovacs, and B. Müller, 'Designing micro- and nanostructures for artificial urinary sphincters', San Diego, California, Apr. 2012, p. 83400A. doi: 10.1117/12.914649.

[15] L. Paternò, G. Tortora, and A. Menciassi, 'Hybrid Soft–Rigid Actuators for Minimally Invasive Surgery', *Soft Robot.*, vol. 5, no. 6, pp. 783–799, Dec. 2018, doi: 10.1089/soro.2017.0140.

[16] M. De Volder and D. Reynaerts, 'Pneumatic and hydraulic microactuators: a review', *J. Micromechanics Microengineering*, vol. 20, no. 4, p. 043001, Apr. 2010, doi: 10.1088/0960-1317/20/4/043001.

[17] S. Li, D. M. Vogt, D. Rus, and R. J. Wood, 'Fluid-driven origami-inspired artificial muscles', *Proc. Natl. Acad. Sci.*, vol. 114, no. 50, pp. 13132–13137, Dec. 2017, doi: 10.1073/pnas.1713450114.

[18] S. Li *et al.*, 'A Vacuum-driven Origami "Magic-ball" Soft Gripper', in *2019 International Conference on Robotics and Automation (ICRA)*, Montreal, QC, Canada, May 2019, pp. 7401–7408. doi: 10.1109/ICRA.2019.8794068.

[19] W. Zhao, N. Li, L. Liu, J. Leng, and Y. Liu, 'Origami derived self-assembly stents fabricated via 4D printing', *Compos. Struct.*, vol. 293, p. 115669, Aug. 2022, doi: 10.1016/j.compstruct.2022.115669.

[20] C. S. Kothera, M. Jangid, J. Sirohi, and N. M. Wereley, 'Experimental Characterization and Static Modeling of McKibben Actuators', *J. Mech. Des.*, vol. 131, no. 9, p. 091010, Sep. 2009, doi: 10.1115/1.3158982.

[21] R. T. Kershen, K. M. Azadzoi, and M. B. Siroky, 'Blood flow, pressure and compliance in the male human bladder', *J. Urol.*, vol. 168, no. 1, pp. 121–125, Jul. 2002.

[22] M. H. Ho and N. N. Bhatia, 'CHAPTER 51 - Lower Urinary Tract Disorders in Postmenopausal Women', in *Treatment of the Postmenopausal Woman (Third Edition)*, R. A. Lobo, Ed. St. Louis: Academic Press, 2007, pp. 693–737. doi: 10.1016/B978-012369443-0/50063-6.

[23] E. T. Roche *et al.*, 'A Bioinspired Soft Actuated Material', *Adv. Mater.*, vol. 26, no. 8, pp. 1200–1206, Feb. 2014, doi: 10.1002/adma.201304018.

[24] W. Felt, M. A. Robertson, and J. Paik, 'Modeling vacuum bellows soft pneumatic actuators with optimal mechanical performance', in *2018 IEEE International Conference on Soft Robotics (RoboSoft)*, Livorno, Apr. 2018, pp. 534–540. doi: 10.1109/ROBOSOFT.2018.8405381.

[25] F. Arab Hassani, H. Jin, T. Yokota, T. Someya, and N. V. Thakor, 'Soft sensors for a sensing-actuation system with high bladder voiding efficiency', *Sci. Adv.*, vol. 6, no. 18, p. eaba0412, May 2020, doi: 10.1126/sciadv.aba0412.

[26] AMS - Men's Health, 'AMS Conceal Reservoir brochure'. Sep. 2016. Accessed: Jan. 03, 2022. [Online]. Available: https://www.amsmenshealth.com/content/dam/bostonscientific/uro-wh/general/ams/Resources/MH-402906-AA_Conceal%20Physician%20Sell%20Sheet-final.pdf